ACS chemical biology

ARTICLES

pubs.acs.org/acschemicalbiology

Zinc Sparks Are Triggered by Fertilization and Facilitate Cell Cycle Resumption in Mammalian Eggs

Alison M. Kim,[†,‡] Miranda L. Bernhardt,[†] Betty Y. Kong,[†] Richard W. Ahn,[‡,§] Stefan Vogt,[⊥] Teresa K. Woodruff,[†,‡,¶,*] and Thomas V. O'Halloran[‡,§,¶,*]

[†]Department of Obstetrics and Gynecology, Feinberg School of Medicine, Northwestern University, 250 E. Superior St., Suite 3-2303, Chicago, Illinois 60611, United States

[‡]The Chemistry of Life Processes Institute and [§]Department of Chemistry, Northwestern University, 2145 Sheridan Rd., Evanston, Illinois 60208, United States

[⊥]X-ray Science Division, Argonne National Laboratory, 9700 S. Cass Ave., Argonne, Illinois 60439, United States

[¶]Department of Molecular Biosciences, Northwestern University, 2205 Tech Drive, Hogan 2-100, Evanston, Illinois 60208, United States

Supporting Information Web-Enhanced

ABSTRACT: In last few hours of maturation, the mouse oocyte takes up over twenty billion zinc atoms and arrests after the first meiotic division, until fertilization or pharmacological intervention stimulates cell cycle progression toward a new embryo. Using chemical and physical probes, we show that fertilization of the mature, zinc-enriched egg triggers the ejection of zinc into the extracellular milieu in a series of coordinated events termed zinc sparks. These events immediately follow the well-established series of calcium oscillations within the activated egg and are evolutionarily conserved in several mammalian species, including rodents and nonhuman primates. Functionally, the zinc sparks mediate a decrease in intracellular zinc content that is necessary for continued cell cycle progression, as increasing zinc levels within the activated egg results in the reestablishment of cell cycle arrest at metaphase. The mammalian egg thus uses a zinc-dependent switch mechanism to toggle between metaphase arrest and resumption of the meiotic cell cycle at the initiation of embryonic development.

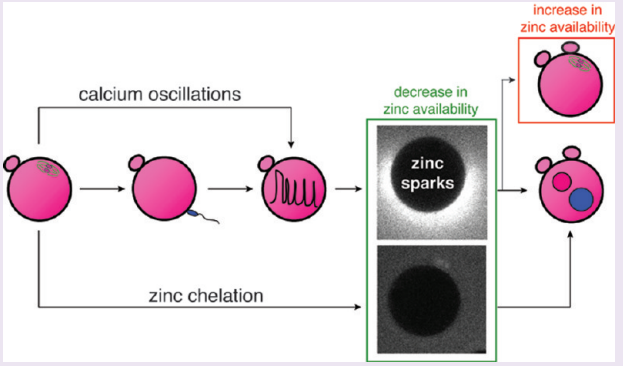

The biological functions of metal ions have traditionally been thought to be limited to structural and catalytic roles within proteins. The alkaline earth metal calcium is one metal in biology for which there are well-established signaling functions. Periodic elevations in the intracellular concentration of free calcium ions, also known as calcium transients or oscillations, are readily detected using fluorescent probes and are known to drive a number of biological processes (reviewed in ref 1). This is perhaps best illustrated in the egg, where repetitive calcium transients are among the earliest observable events after fertilization.[2] Several parameters of these calcium transients, including total number, frequency, and amplitude influence which downstream developmental events are initiated.[3−5] These cellular processes, which include cortical granule (CG) exocytosis[6,7] and cell cycle progression,[8,9] can be initiated in the absence of sperm by stimulatory agents that induce parthenogenesis.[10−13] Interestingly, the normal pattern of calcium oscillations is disrupted in eggs matured under conditions that limit the availability of the transition metal zinc,[14] suggesting that the physiologies of these metals are somehow connected in the egg.

In a departure from its well-established role as an enzymatic cofactor or structure-stabilizing agent, fluctuations in the total concentration of intracellular zinc have recently been shown to contribute to the proper cell cycle regulation in maturing oocytes. Intracellular zinc levels increase by more than 50% and over 10^{10} atoms per cell are accrued during the final stage of oocyte maturation, also known as meiotic maturation.[14] This significant cellular metal accumulation event occurs over a remarkably short time interval and is a physiological imperative, as insufficient accumulation of zinc leads to a premature meiotic arrest at telophase I instead of metaphase II.[14] This zinc-dependent meiotic checkpoint arises, in part, because zinc-insufficient eggs fail to reestablish maturation promoting factor (MPF) activity,[15] which is necessary for eggs to set up and maintain meiotic arrest at metaphase II. These results revealed a previously unrecognized role for zinc in cell cycle switching events, namely, the regulation of meiotic progression in the egg.

Received: March 14, 2011
Accepted: April 13, 2011
Published: April 28, 2011

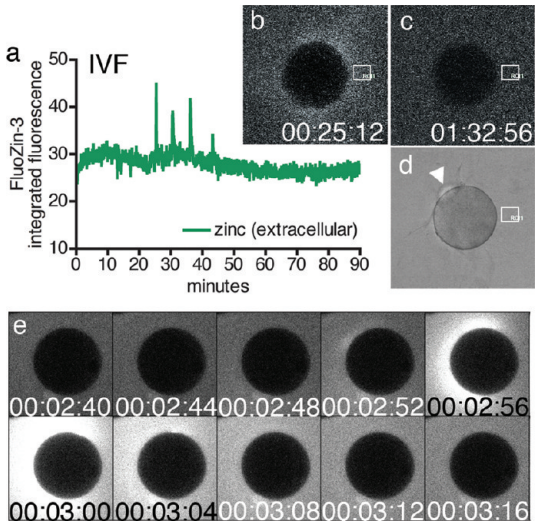

Figure 1. Zinc is released into the extracellular environment as an early fertilization event. Changes in extracellular zinc concentration are readily monitored with FluoZin-3 during *in vitro* fertilization, and rapid, repetitive increases in fluorescence intensity were detected (a) by ROI analysis (denoted by white boxes in b–d). Each zinc spark can be distinguished in the time-lapse series (b, 00:25:12) against background fluorescence (representative example in c, 01:32:56). Successful fertilization was confirmed by the extrusion of a second polar body (d). Zinc sparks were also noted during strontium chloride induced parthenogenesis (e, 00:02:56). Time is expressed as hh:mm:ss, wherein 00:00:00 represents the start of image acquisition.

Given this role for zinc in the maturing oocyte, we explored whether this function extended to cell cycle regulation in the fertilized egg. We first investigated the dynamics of zinc and calcium within the physiological context of fertilization using a variety of chemical probes that can report changes in the concentration of labile and loosely bound zinc ions and discovered that the calcium oscillations induced a rapid ejection of zinc through an event termed the zinc spark. We show that zinc sparks are evolutionarily conserved in three mammalian species and that these fluxes in intracellular zinc availability mediate cell cycle resumption. Together with our previous reports on zinc in the maturing oocyte, we describe herein a new zinc-dependent mechanism for cell cycle regulation in the mammalian egg.

RESULTS AND DISCUSSION

Release of Zinc at Egg Activation Is a Conserved Event in Mammalian Species. Extracellular zinc events were monitored during fertilization of mouse eggs using a membrane-impermeant derivative of the zinc fluorophore FluoZin-3.[16] Strikingly, fertilization triggered the repetitive release of zinc into the extracellular milieu (Figure 1a,b). These events were termed zinc sparks for their brevity and intensity. Successful fertilization was confirmed by extrusion of the second polar body (Figure 1c,d, PB2). These events were recapitulated during parthenogenesis of mouse eggs (Figure 1e, Video S1). Importantly, zinc sparks are an evolutionarily conserved phenomenon, as they were also observed during parthenogenetic activation of two different nonhuman primate species, *Macaca mulatta* (rhesus macaque) and *Macaca fascicularis* (crab-eating macaque) (Supplementary Figure S1, Video S2). Additional characterization of the zinc sparks was completed using parthenogenetically activated mouse eggs.

The dynamics of the zinc sparks were variable from egg to egg. Zinc sparks occurred during the first 90 min of activation, and individual eggs exhibited between one and five zinc sparks, which were counted in a plot of fluorescence intensity over time (see representative plot in Figure 1a). Eighty-one percent of all eggs examined ($N = 28$) exhibited two or three exocytosis events, while 11% exhibited one event and 8% exhibited four or five events. No more than five zinc sparks were observed in any of the samples. The interval between each exocytic event was 9.5 ± 0.8 min (mean ± SEM, $N = 36$), although the range of intervals was quite broad, between 3.46 and 26.00 min.

It is notable that the zinc sparks could be induced by fertilization or by parthenogenesis using two different reagents: strontium chloride in rodents and ionomycin in two nonhuman primate species. Strontium chloride induces multiple calcium transients,[6] whereas ionomycin induces only a single calcium transient.[17] Accordingly, multiple zinc sparks were observed in rodents, whereas only a single zinc spark was seen in the nonhuman primate species. This result speaks to a possible calcium dependence of the zinc sparks, and this was further investigated in the following experiments.

Initiation of the Zinc Sparks Is Dependent on Intracellular Calcium Transients. To understand the role of zinc sparks within the temporal context of the calcium oscillations, we simultaneously monitored intracellular calcium oscillations alongside zinc sparks using the acetoxymethyl ester (AM) derivative of the calcium fluorophore Calcium Green-1 (ex 506, em 531), which has excitation and emission spectra similar to those of FluoZin-3 (Figure 2a, Video S3). Each zinc spark was closely associated with an intracellular calcium transient (Figure 2b); upon closer inspection, it was found that each zinc spark was immediately preceded by an elevation in intracellular calcium (Figure 2c). Parallel experiments employing a membrane permeable zinc fluorophore, FluoZin-3 AM did not reveal clear intracellular zinc transients (Supplementary Figure S2a), ruling out the possibility that large oscillations in intracellular free zinc contributes to the intracellular transients detected by Calcium Green-1 AM We confirmed that this was representative of successfully activated eggs by simultaneously monitoring second polar body (PB2) extrusion by brightfield imaging (Supplementary Figure S2a). Further control experiments employing one fluorophore at a time reveal that the zinc sparks are not dependent upon or affected by the presence of the calcium probe; for example, detection of zinc sparks using FluoZin-3 in the absence of Calcium Green-1 AM is shown in Figure 1a (fertilization) and Figure 1e (parthenogenesis).

The observation that calcium transients immediately preceded each zinc release event supports the idea that the zinc sparks were directly dependent on intracellular calcium fluxes. Two lines of evidence provided additional support. First, zinc sparks did not occur in the absence of an activating agent and, hence, a lack of calcium oscillations (Supplementary Figure S2b). Second, zinc sparks were absent in eggs treated with the membrane-permeable acetoxymethyl ester (AM) derivative of 1,2-bis(*o*-aminophenoxy)-ethane-*N*,*N*,*N*′,*N*′-tetraacetic acid (BAPTA). This reagent is commonly used to suppress calcium oscillations in eggs,[6,7] and as such, both calcium transients and zinc sparks were absent in BAPTA AM-treated eggs even after extended culture in strontium chloride (Supplementary Figure S2c). Furthermore, these eggs did not extrude a second polar body or form a pronucleus

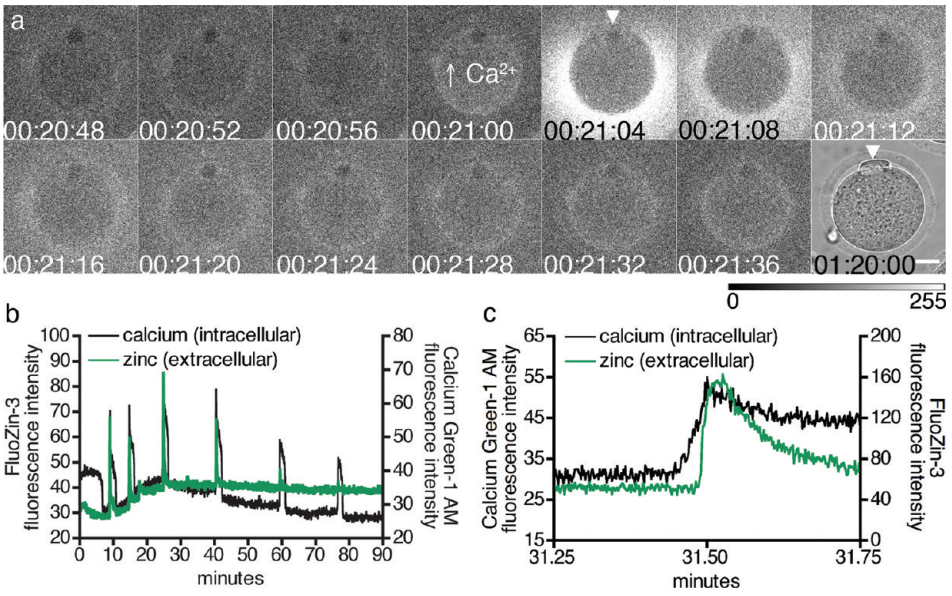

Figure 2. Zinc sparks are polarized and are immediately preceded by intracellular calcium transients. Shortly following activation, zinc sparks occur around the egg cortex with the exception of a zinc-spark-free region (a, 00:21:04, arrowhead). This spark-free region corresponds to the region containing the meiotic spindle, where the second polar body is extruded (a, 01:20:00, arrowhead). Egg activation was confirmed by simultaneously monitoring intracellular calcium oscillations with Calcium Green-1 AM every 4 s (b). Intracellular calcium increases immediately before a zinc spark, as evident when images were collected at a faster acquisition rate of every 100 ms in an independent experiment (c). Time is expressed as hh:mm:ss, wherein 00:00:00 represents the start of image acquisition. In all cases, extracellular zinc was detected with FluoZin-3.

(Supplementary Figure S2d,e). Taken together, these data indicate that the zinc sparks are preceded by and may depend upon the calcium oscillations that begin early in the egg activation process.

Localization of Zinc Is Cortically Polarized in Mature Eggs. We noted that the zinc sparks were excluded from the region corresponding to the location of the meiotic spindle, as confirmed by the extrusion of the second polar body at that site (Figure 2a, arrowheads). To investigate possible cellular sources of the zinc release, the distribution of zinc was determined in unfertilized eggs by synchrotron-based X-ray fluorescence microscopy (XFM). This technique provides the localization and abundance of the total zinc content of a sample, including both the loosely bound (labile or chelatable) and tightly bound cellular pools, and was previously used to quantify zinc and other transition metals in maturing oocytes.[14] The XFM images revealed distinct regions of high zinc concentration that formed a polarized and hemispherical pattern (Figure 3a; i–iii represent three independent samples). Other essential transition metals such as iron exhibit a homogeneous distribution across the entire cell (Figure 3b; i-iii represent three independent samples). Quantitative analysis revealed that zinc was an order of magnitude more abundant than either iron or copper at all points between the mature, *in vivo* ovulated (IVO) MII stage egg and the two-cell embryo (24 h post-fertilization, or hpf). There is a downward trend with a mean loss of about six billion atoms of zinc upon fertilization, and this trend continued at 6 and 24 hpf (Supplementary Figure S3). Assuming different standard deviations for each elemental group, ANOVA analysis noted a significant difference in the mean zinc content across the four time points (p = 0.019 for zinc). We also confirmed by fluorescence imaging of intracellular zinc that chelatable zinc, as detected by FluoZin-3 AM also decreased in activated eggs following the zinc sparks (Supplementary Figure S4).

We next asked whether the polarized pattern for total zinc correlated with the distribution of labile (or chelator-accessible) zinc in the egg. Two chemically distinct, zinc-selective fluorophores were used to visualize this loosely bound zinc in live, unfertilized eggs. Projected images of confocal Z-stack series revealed that zinc fluorescence was concentrated away from the meiotic spindle, which was marked with fluorescent DNA probes (Figure 3c–h). This was also evident when analyzing the Z-series slice by slice, which clearly illustrated higher cortical localization of zinc relative to the cytoplasm (Supplementary Figure S5). Furthermore, zinc was present in distinct intracellular compartments as indicated by punctate foci of fluorescence. This pattern was independent of the molecular properties of the zinc probe: both Zinquin ethyl ester (Figure 3c) and FluoZin-3 AM (Figure 3f) yielded the same general pattern wherein a majority of the foci have a peripheral localization. These probes have pM values of 9.3[18] and 8.8,[16] respectively, where pM = −log[M] when [L] = 10 μM and [M] = 1 μM at pH 7.4.[19] Given that the pM values of zinc-binding metalloproteins are significantly higher (for example, carbonic anhydrase has a pM value of 12.4[18]), it is unlikely that the probes are detecting zinc tightly bound to metalloproteins. Rather, these and related fluorescent chelators compete by mass action for zinc ions that are otherwise weakly bound to biopolymers and low molecular weight compounds. Some of the latter have been proposed to buffer intracellular zinc concentrations in various compartments.[20,21] While the zinc pools in different compartments of eukaryotic cells are not well understood in either kinetic and thermodynamic terms, the fluorescent probes are generally thought to be delineating compartments with elevated concentrations of "chelator-accessible" zinc ions.[22,23] In addition to their punctate distribution, the pools of chelator-accessible zinc were concentrated toward the vegetal pole and away from the meiotic spindle, whose location was marked with live-cell nuclear stains Syto 64 (Figure 3d) or

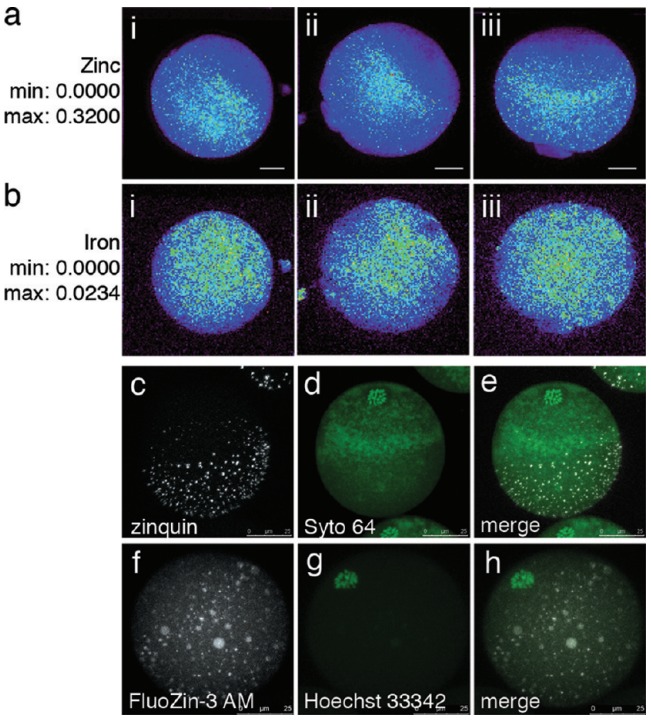

Figure 3. Zinc ions are cortically polarized in the mouse egg. Total zinc, as detected by synchrotron-based X-ray fluorescence (a, b), is uniquely polarized in the unfertilized egg (a; i−iii represent replicates). This distribution is absent in the other essential transition elements, such as iron (b; i−iii represent replicates). The minimum and maximum range of each group of images are given units of $\mu g/cm^2$. Labile (chelator-accessible) zinc, as detected by confocal microscopy (c−h), also has a hemispherical distribution in the live egg, as detected by two chemically distinct zinc fluorophores: zinquin ethyl ester (c−e) and FluoZin-3 AM (f−h). Co-staining with a DNA marker (Syto 64 in d, Hoechst 33342 in g) revealed that zinc was concentrated at the vegetal pole away from the meiotic spindle. The images depicted here are projected images of the complete Z-series; representative slices from these same Z-stacks confirming cortical localization of zinc are shown in Figure S5 in Supporting Information. Scale bar = 20 μm (a, b) or 25 μm (c−h).

Hoechst 33342 (Figure 3g) as seen in the merged images (Figure 3e and h). The polarized distribution detected both by the zinc fluorophores and by XFM corroborates a significant cortical compartmentalization of zinc in the egg. Since the polarized distribution of labile zinc mirrors the polarized release of zinc during the zinc sparks, it is likely that some fraction of these zinc-enriched compartments act the source of the coordinated zinc release events, *i.e.*, the zinc sparks.

The polarization of the zinc-enriched compartments mirrors that of the cortical granules (CG), which are exocytic vesicles that participate in the cortical reaction, which involves the hardening of the zona pellucida to establish a block to polyspermy at fertilization.[24] We hypothesized that the zinc sparks would mirror the mechanisms regulating the cortical reaction and first investigated whether the zinc sparks were the product of an exocytic event. To inhibit exocytosis, eggs were treated with cytochalasin B (CytoB), an agent that disrupts actin reorganization and has previously been shown to disrupt CG exocytosis in mouse and hamster eggs.[7,25] CytoB-treated eggs still undergo normal calcium oscillations upon activation but exhibit only a single zinc spark concomitantly with the first calcium transient (Supplementary Figure S6). In most cases, subsequent sparks were inhibited (Supplementary Figure S6). It is likely that a cohort of the zinc-containing vesicles is prefused with the egg membrane, allowing the first spark to occur even in the presence of CytoB. This type of phenomenon has been described for cortical granules in the sea urchin egg, where one subset of CGs are in a hemifused state prior to activation.[26]

To determine whether the zinc sparks participate in zona hardening like the cortical reaction, we utilized a zinc-insufficient egg model that was obtained by treating oocytes with the heavy metal chelator TPEN during *in vitro* maturation.[14] These eggs did not undergo zinc sparks, even when activated in the same dish as control eggs (Video S4). We previously reported that these zinc-insufficient eggs fertilize at rates comparable to control eggs. Additionally, zinc-insufficient eggs form the normal number of pronuclei, as indicated by the presence of only one male and one female pronucleus.[14] Therefore, we find no evidence that the zinc sparks participate in the block to polyspermy.

Meiotic Resumption at Egg Activation Is Dependent on the Zinc Sparks. The zinc-insufficient egg model revealed a critical function for zinc in the proper establishment of cell cycle arrest in the mature egg,[14] which was supported by the observation that chelation of zinc initiated egg activation.[27] Given these results, we considered the possibility that a decrease in bioavailable zinc was necessary to permit downstream developmental events upon egg activation. To address this possibility, we treated activated eggs with zinc pyrithione (ZnPT), a zinc ionophore that elevates the intracellular free zinc content of mammalian cells.[28] First, we performed a titration on unfertilized eggs and did not observe cytotoxic effects until concentrations of ZnPT reached 50 μM (Supplementary Figure S7). To minimize such cytotoxic effects, a 5-fold lower concentration of ZnPT (10 μM) was used for subsequent experiments. Eggs were subjected to a 10 min ZnPT treatment after the completion of the zinc sparks at 1.5 h postactivation (hpa) (Figure 4a). Control (untreated) and ZnPT-treated eggs were then cultured until pronuclear formation was observed in the control group (6−8 hpa; Figure 4b,c). Ninety percent of control eggs formed an organized pronucleus that was visible by brightfield (Figure 4b, arrowheads) and also by fluorescence (Figure 4d). F-actin was homogeneous around the cell (Figure 4e), and α-tubulin was compact in a spindle remnant (Figure 4f) between the egg and the second polar body (merged image in Figure 4g).

In contrast, only 17% of ZnPT-treated eggs formed a pronucleus; the majority did not have a pronuclear structure that was clearly visible by brightfield (Figure 4c). In 84% of these eggs lacking a pronucleus, we noted the presence of aligned chromosomes (Figure 4h), instead of the membrane-enclosed nucleus observed in the control eggs. Notably, we also observed an actin-enriched region in the ZnPT-treated eggs (Figure 4i, arrow) at the cortical region overlying the chromosomes (Figure 4j). This "actin cap" is a polarized feature thought to be unique to unfertilized eggs.[29,30] Most strikingly, the chromosomes and α-tubulin (Figure 4j) were organized into a metaphase-like spindle (merged image in Figure 4k), which resembled a freshly ovulated, MII-arrested egg (Figure 4l−o). It should be noted that only eggs with a clear second polar body were selected for ZnPT treatment; thus, the spindle configuration in ZnPT-treated activated eggs, while metaphase-like, is not that of metaphase II. An analogous metaphase-like spindle and arrest has been seen in parthenogenetically activated rodent eggs that receive insufficient activating stimulus: such cells complete meiosis II but stall

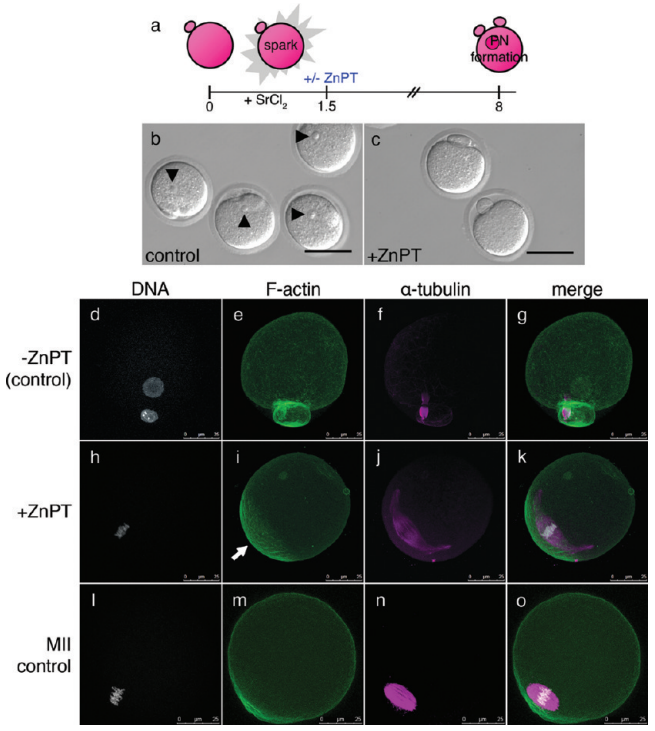

Figure 4. Sustained elevation of intracellular zinc availability following egg activation leads to reestablishment of metaphase arrest. Eggs were activated with strontium chloride ($SrCl_2$) then treated with zinc pyrithione (ZnPT) 1.5 h later (a). At 6 h postactivation, control eggs form pronuclei (b, arrowheads), whereas the majority of eggs treated with ZnPT do not (c). When visualized by fluorescence, control eggs display decondensed DNA organized within a defined nucleus (d). F-actin is homogeneous around the egg's cortex (e), and α-tubulin remains organized as a spindle midbody remnant (f), which is visible between the egg and the second polar body (g, merged image). In contrast, ZnPT-treated eggs display condensed chromosomes (h) adjacent to an area of concentrated, cortical F-actin (i). α-tubulin is organized in a metaphase-like configuration (j) around the chromosomes (k, merged image). This layout mirrors the subcellular arrangement in unfertilized eggs (l–o), which also display condensed chromosomes (l) overlaid with an actin cap (m), surrounded by a metaphase spindle (n). Scale bar = 80 μm (b, c) or 25 μm (d–o).

at a so-called third metaphase (MIII) instead of progressing to interphase.[15,19]

In the reverse of the zinc-loading experiment, the intracellular availability of zinc in the egg was decreased by continuous culture in the presence of 10 μM TPEN; we previously confirmed the specificity of this chelator for zinc in mouse oocytes.[14] After 8 h of culture, most control eggs maintained metaphase II arrest while those exposed to TPEN had a pronucleus-like structure at significantly higher rates (Supplementary Figure S8). A similar observation was made by Suzuki and colleagues with much higher concentrations of TPEN, and they further reported that other heavy metal chelators, including *p*-aminosalicylic acid, ammonium tetrathiomolybdate, and 2,2′-bipyridine, were unable to cause egg activation,[27] thus speaking to the unique role of zinc in driving this process. These complementary experiments support the idea that a significantly elevated zinc quota is associated with metaphase arrest and that the coordinated exocytosis of zinc upon egg activation relieves this arrest. Furthermore, these results also distinguish the intracellular target of the calcium-selective chelator BAPTA AM (Supplementary Figure S2) from that of TPEN. Given that BAPTA is also known to have a substantial affinity for zinc[31−33] (K_d = 107 nM for Ca^{2+} and 8 nM for Zn^{2+}), a potential question is whether the BAPTA AM treatment is influencing zinc- or calcium-dependent intracellular processes. At the 10 μM concentration used in our studies, BAPTA and TPEN had significantly different effects on egg physiology. This is illustrated by the fact that long-term exposure to BAPTA did not parthenogenetically activate eggs (Supplementary Figure S2) but TPEN did (Supplementary Figure S8). Under these conditions, we conclude that BAPTA is scavenging intracellular free calcium and thereby blocking calcium oscillations. Taken together, the results support a model in which the calcium oscillations initiate and are required for the programmed loss of cellular zinc via the zinc sparks and that in turn drives cell cycle resumption.

Summary. It was previously suggested that only a modulation of intracellular zinc, not calcium, was essential for the resumption of the cell cycle following egg activation.[27] In contrast, we show here that within the physiological context of fertilization, calcium transients immediately precede each zinc spark event. These apparently paradoxical results can be explained as thus: both studies achieve a decrease in the intracellular bioavailability of zinc but through different means (summarized in Figure 5). Whereas we reached this end point through a physiological means, the calcium-triggered zinc spark, the previous report bypassed the need for a calcium-dependent event by artificially lowering zinc availability within the mature egg via TPEN treatment.[27] Thus, we conclude that the calcium transients are involved in the physiological mechanism by which the lowering of intracellular zinc availability is initiated, namely, by inducing the zinc sparks and permitting cell cycle resumption to occur. One way that this change in the intracellular zinc status may regulate the cell cycle is by affecting the activity of the anaphase promoting complex/cyclosome (APC/C) inhibitor Emi2 (early mitotic inhibitor-2), which has been shown to be important for the establishment of metaphase II arrest[34] and contains a conserved zinc-binding region that is required for activity.[20] Although we have reported trends in the egg's total zinc content pre- and postfertilization, additional studies are required to define these vital fluxes in greater detail. Methods that quantify changes in the subset of the total zinc pool that is compartmentalized, labile, and/or subject to modulation in response to egg activation will provide greater mechanistic insight in conjunction with the pathways that are activated at the protein level.

We postulate that in the egg, intracellular zinc fluxes play a gatekeeping role between cell cycle arrest and resumption and that this pathway is controlled in part by intracellular calcium signaling (Figure 5). Ultimately, the fertilized mammalian oocyte faces a physiological imperative to lower intracellular zinc availability in order to permit cell cycle resumption, and this is achieved in part via the calcium-regulated zinc sparks. Indeed, the same effect can be achieved pharmacologically through the intracellular chelation of zinc.[27] Importantly, the abundance of zinc appears to act as both a permissive factor and a maintenance factor in metaphase arrest. During oocyte maturation, an elevated level of zinc must be accumulated to establish metaphase arrest.[14] Conversely, during egg activation, the zinc sparks are used to decrease bioavailable zinc, but metaphase arrest can be reestablished if the levels of intracellular zinc are raised. These results implicate zinc as a key regulatory element in egg activation and are consistent with a specialized role for this transition metal in

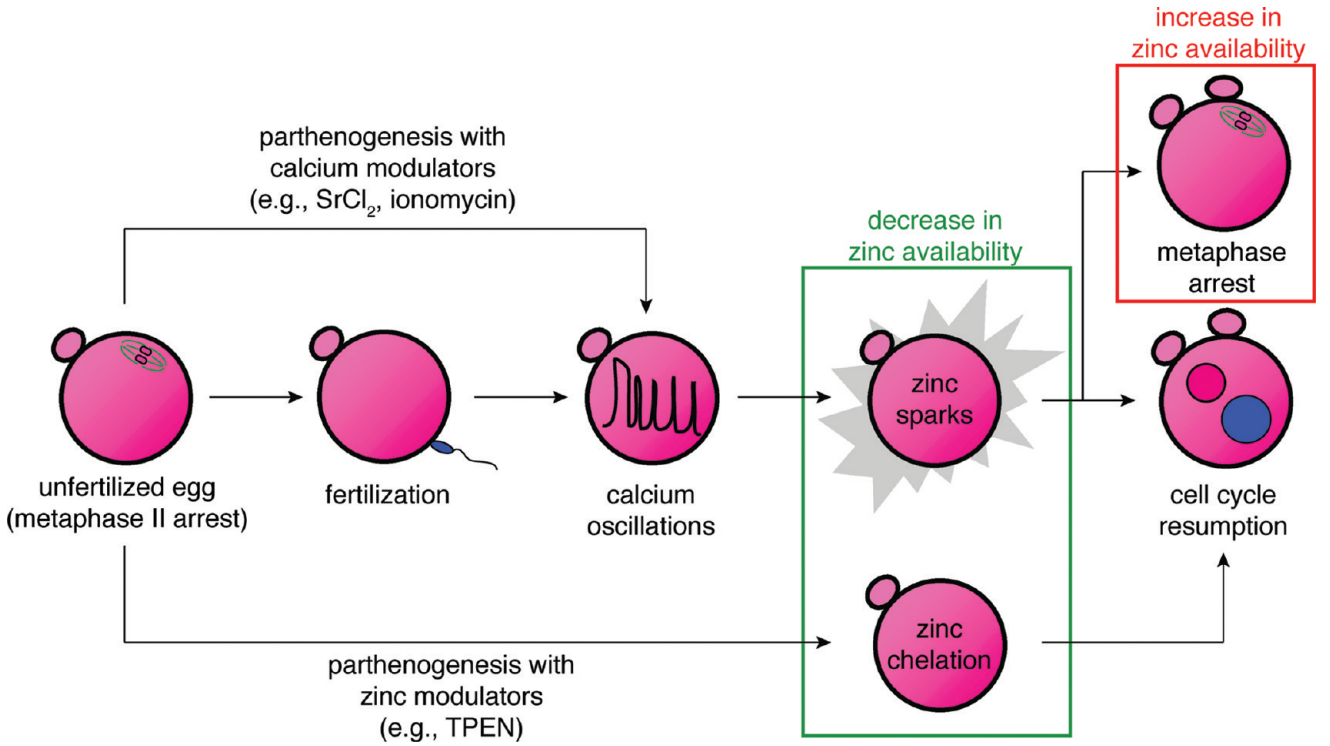

Figure 5. Zinc plays a gatekeeping role, switching between cell cycle arrest and resumption. The unfertilized egg can now be activated by three different approaches, all of them leading to a decrease in intracellular zinc availability. The first is through the physiological pathway, fertilization (center row). This induces calcium oscillations in the egg, leading to the zinc sparks and subsequent cell cycle resumption. The two other approaches induce parthenogenesis and are pharmacological, either using modulators of intracellular calcium (top arrow) or zinc (bottom arrow). The calcium-based approaches induce zinc sparks, while the zinc-based approach bypasses the need for calcium oscillations by directly decreasing the availability of zinc in the egg (green box). Furthermore, cell cycle arrest at metaphase can be reestablished by raising zinc availability (red box), thus implicating zinc as a central regulator of the cell cycle during oocyte maturation and fertilization.

the regulation of developmental processes during the earliest stages of life.

MATERIALS AND METHODS

Mouse Egg Collection. Eggs were collected from adult (6−8 weeks old) female mice of the CD-1 strain. Mice were superstimulated with an i.p. injection of 5 IU of pregnant mare's serum gonadotropin (PMSG, EMD Biosciences, San Diego, CA), followed 46−48 h later by an i.p. injection of 5 IU human chorionic gonadotropin (hCG, Sigma-Aldrich, St. Louis, MO). Mice were sacrificed by CO_2 asphyxiation and cervical dislocation 13−14 h post-hCG administration. Clutches of cumulus-oocyte complexes were isolated from the oviducts. Cumulus cells were denuded using 30 μg/mL hyaluronidase and gentle aspiration through a narrow-bore pipet. Animals were treated in accord with the National Institutes of Health Guide for the Care and Use of Laboratory Animals. Food and water were given ad libitum. The Northwestern University Institutional Animal Care and Use Committee (IACUC) approved all protocols.

Time-Lapse Imaging of Mouse Eggs during *in Vitro* Fertilization. Sperm from the cauda epididymides of proven breeder CD-1 males were used for sperm *in vitro* fertilization (IVF). The sperm population was purified using Percoll gradient centrifugation (PGC) as described previously[35] and capacitated for up to 3 h in IVF medium composed of potassium simplex optimized medium (KSOM, Millipore, Billerica, MA) supplemented with 3 mg/mL bovine serum albumin (BSA, MP Biomedicals, Solon, OH) and 5.36 mM D-glucose (Sigma-Aldrich). Superovulated eggs were collected as described above. The zona pellucida (ZP) was removed by brief treatment in acidic Tyrode's solution (pH 2.5, Millipore). The ZP-free eggs were allowed to settle in a 50 μL drop of calcium- and magnesium-free Dulbecco's PBS (DPBS, Invitrogen, Carlsbad, CA) on a glass-bottom dish (Bioptechs Inc., Butler, PA) coated with poly-L-lysine. After 10 min, IVF medium containing 20 μM FluoZin-3 (Invitrogen) was slowly added to a final volume of 1 mL, taking care not to disturb the eggs. The final DMSO concentration was 0.1% (v/v), as higher concentrations were cytotoxic to sperm. Capacitated sperm were added to the eggs to a final concentration of 1.0×10^6 sperm/mL, and image acquisition began immediately upon addition of sperm. Images were acquired every 4 s for a total duration of 3 h. All images were acquired on a TCS SP5 confocal microscope (Leica Microsystems, Heidelberg, Germany) equipped with a stage top incubator (Tokai Hit, Shizuoka, Japan), 20x objective, and an Ar (488 nm) laser line.

Parthenogenetic Activation and Pyrithione Treatment of Mouse Eggs. Strontium chloride ($SrCl_2$) was prepared as a 1 M stock solution in calcium-free KSOM (Millipore) and stored as ready-to-use aliquots at −20 °C. $SrCl_2$ was diluted to a working concentration of 10 mM in calcium-free KSOM. Eggs were incubated in $SrCl_2$ for 90 min. In some cases, eggs were then treated with zinc pyrithione (ZnPT, Sigma-Aldrich). Dose−response experiments were performed to test cytotoxicity; a distinct cytotoxic effect was seen at concentrations above 20 μM. Therefore, ZnPT concentrations were reduced to 10 μM, and treatment time was limited to 10 min at 37 °C in an atmosphere of 5% CO_2. Both control and ZnPT-treated eggs were washed and transferred to fresh KSOM for extended culture.

Nonhuman Primate Oocyte Collection, *in Vitro* Maturation, and Parthenogenetic Activation. Ovarian tissue was surgically dissected from *Macaca mulatta* (rhesus macaque, 3 years old) and

Macaca fascicularis (crab-eating macaque, 3 years old) females at the Panther Tracks Learning Center (Immokalee, FL). The tissue was cut in half, placed in 15 mL of SAGE oocyte washing medium (Cooper Surgical, Trombull, CT), and shipped overnight at ambient temperature. The tissue was processed within 18 h of surgery. Large follicles were opened by grazing with an insulin-gauge needle. Oocytes of diameter greater than 100 μm (including the zona pellucida) were collected for *in vitro* maturation (IVM), whether they were enclosed by cumulus cells or denuded. They were placed in an IVM medium composed of SAGE oocyte maturation medium (Cooper Surgical) supplemented with 75 mIU/μL follicle stimulating hormone (FSH, a gift from Organon, Roseland, NJ), 75 mIU/μL luteinizing hormone (LH, a gift from Ares Serono, Randolph, MA), 1.5 IU/μL hCG (Sigma-Aldrich), and 5 ng/mL epidermal growth factor (EGF, BD Biosciences, San Jose, CA). Oocytes were observed up to 48 h postmaturation and used immediately for imaging upon complete extrusion of a polar body.

Time-Lapse Imaging of Parthenogenetically Activated Eggs. Eggs were first incubated in 10 μM Calcium Green-1 AM (Invitrogen) and 0.04% (w/v) Pluronic F-127 (Invitrogen) for either 30 min (mouse) or 60 min (nonhuman primate) at 37 °C. Mouse eggs were washed in calcium-free KSOM (Millipore) and transferred to a 50 μL drop containing 10 mM $SrCl_2$ (Sigma-Aldrich) and 50 μM FluoZin-3 (Invitrogen) on a glass-bottom dish (Bioptechs Inc.). Nonhuman primate eggs were transferred to one end of a long and shallow drop (20 μL) of calcium-free KSOM (Millipore) containing 50 μM FluoZin-3 (Invitrogen) on a glass-bottom dish (Bioptechs Inc.), covered with oil for embryo culture (Irvine Scientific, Santa Ana, CA). Ionomycin was perfused in at the opposite end to a final concentration of 20 μM. In both cases, image acquisition began immediately and occurred every 4 s for a total of 1−3 h (mouse) or 15 min (nonhuman primate), unless noted otherwise. All images were acquired on a TCS SP5 confocal microscope (Leica Microsystems) equipped with a stage top incubator (Tokai Hit), 20x objective, and an Ar (488 nm) laser line.

Imaging of Total and Labile Zinc in the Mouse Egg. Fertilized eggs were collected at 2 and 6 hpf were prepared whole-mount for synchrotron-based X-ray fluorescence microscopy (XFM). Cells were transferred with a minimal amount of media to an intact 5 mm × 5 mm silicon nitride window (Silson, Blisworth, U.K.) on a heated stage warmed to 37 °C. When most of the media had evaporated without drying out the sample, 1 μL of ammonium acetate solution (100 mM, 4 °C) was administered to each sample under a dissection microscope. This facilitated a quick wash and dehydration process, leaving the morphology of the sample intact without causing membrane rupture. XFM was performed at Beamline 2-ID-E at the Advanced Photon Source (Argonne National Laboratory, Argonne, IL). Ten keV X-rays were monochromatized with a single bounce Si(111) monochromator, and focused to a spot size of 0.5 μm × 0.6 μm using Fresnel zone plate optics (X-radia, Concord, CA). Raster scans were done in steps of 1 μm. Fluorescence spectra were collected with a 1 s dwell time using a silicon drift detector (Vortex-EM, SII NanoTechnology, CA). Quantification and image processing was performed with MAPS software. The fluorescence signal was converted to a two-dimensional concentration in $\mu g/cm^2$ by fitting the spectra against the thin-film standards NBS-1832 and NBS-1833 (National Bureau of Standards). It was assumed that no elemental content was lost during sample preparation. The data was compared to the total zinc content in unfertilized eggs and two-cell embryos. The data for the two-cell embryo was already published in a previous report.[14] The distribution of labile zinc was interrogated in live, unfertilized mouse eggs using two independent zinc fluorophores, Zinquin ethyl ester (Sigma-Aldrich) and FluoZin-3 AM (Invitrogen). Eggs were incubated in either 20 μM Zinquin ethyl ester in combination with 1 μM Syto 64 (Invitrogen) or 10 μM FluoZin-3 AM in combination with 10 μg/mL Hoechst 33342 (Invitrogen) for 60 min in KSOM (Millipore). They were imaged in 20 μL drops of KSOM covered with oil for embryo culture (Irvine Scientific) on glass-bottom dishes (Bioptechs Inc.). Images were acquired as Z-stacks on a TCS SP5 confocal microscope (Leica Microsystems) equipped with a stage top incubator (Tokai Hit), 63x oil-immersion objective, and HeNe (543 nm), Ar (488 nm), and near-UV (405 nm) laser lines.

TPEN Treatment and Spindle Imaging of Mouse Eggs. Superovulated eggs were collected and transferred to KSOM medium (Millipore) with or without 10 μM TPEN and cultured up to 8 h at 37 °C in an atmosphere of 5% CO_2 in air. Previous work showed that treatment of maturing oocytes with 10 μM TPEN could selectively limit the intracellular acquisition of zinc (relative to iron and copper) but without significant toxicity.[14] Eggs were fixed and permeabilized for 30 min at 37 °C in a solution containing 2% formaldehyde, 2% Triton X-100, 100 mM PIPES, 5 mM $MgCl_2$, and 2.4 mM EGTA. Eggs were then washed and blocked for 1−3 h in 1x PBS containing 0.1 M glycine, 3 mg/mL BSA, 0.01% Tween-20, and 0.01% sodium azide followed by incubation with anti-α-tubulin (1:100, Sigma) in blocking buffer for 1 h at 37 °C. Eggs were washed again in blocking buffer, incubated in Alexa Fluor 488-conjugated goat antimouse IgG (Invitrogen) and rhodamine-phalloidin conjugate (Invitrogen) at 37 °C for 1 h, washed three additional times, and mounted on microscopy slides with coverslips in Vectashield with DAPI. Images were acquired as Z-stacks on a TCS SP5 confocal microscope (Leica Microsystems) equipped with a stage top incubator (Tokai Hit), 63x oil-immersion objective, and HeNe (543 nm), Ar (488 nm), and near-UV (405 nm) laser lines.

Statistical Analysis. The abundance of each element was compared across time points using one-way analysis of variance assuming different standard deviations for each group. These analyses were followed by pairwise comparisons of each time versus each other time using the Tukey-Kramer method.[36] All statistical tests were performed using the software Prism 4.0 (GraphPad Software, San Diego, CA). $P < 0.05$ was considered statistically significant.

■ ASSOCIATED CONTENT

Ⓢ Supporting Information. This material is available free of charge *via* the Internet at http://pubs.acs.org.

Ⓦ Web Enhanced Feature. Video files of zinc spark activity are available in the HTML version of this paper.

■ AUTHOR INFORMATION

Corresponding Author

*E-mail: tkw@northwestern.edu; t-ohalloran@northwestern.edu.

■ ACKNOWLEDGMENT

We are grateful to F. Rademaker for advice on statistical analysis. We thank S. Kiesewetter, J. Jozefik, and D. Mackovic for rodent care and concerns, and Primate Products, Inc. for providing all nonhuman primate tissue. We acknowledge R. Marvin in the Quantitative Bioelement Imaging Center in the Chemistry of Life Processes Institute at Northwestern University for reagents and discussions regarding sample processing. This work is supported by National Institutes of Health Grants P01 HD021921 and GM038784, the W. M. Keck Foundation Medical Research Award, and the Chicago Biomedical Consortium SPARK Award. A.M.K. and R.W.A. are Keck Graduate Scholars. A.M.K. and M.L.B. are fellows of the Reproductive Biology Training Grant (HD007068). R.W.A. is a predoctoral fellow of the CDMRP Breast Cancer Research Program (BC073413). Use of the Advanced Photon Source at Argonne

National Laboratory is supported by the U.S. Department of Energy, Office of Science, Office of Basic Energy Sciences, under Contract No. DE-AC02-06CH11357.

REFERENCES

(1) Berridge, M. J., Bootman, M. D., and Roderick, H. L. (2003) Calcium signalling: dynamics, homeostasis and remodelling. *Nat. Rev. Mol. Cell Biol. 4*, 517–29.

(2) Lawrence, Y., Whitaker, M., and Swann, K. (1997) Sperm-egg fusion is the prelude to the initial Ca2+ increase at fertilization in the mouse. *Development 124*, 233–41.

(3) Ozil, J. P., Banrezes, B., Toth, S., Pan, H., and Schultz, R. M. (2006) Ca^{2+} oscillatory pattern in fertilized mouse eggs affects gene expression and development to term. *Dev. Biol. 300*, 534–44.

(4) Ducibella, T., Huneau, D., Angelichio, E., Xu, Z., Schultz, R. M., Kopf, G. S., Fissore, R., Madoux, S., and Ozil, J. P. (2002) Egg-to-embryo transition is driven by differential responses to Ca^{2+} oscillation number. *Dev. Biol. 250*, 280–91.

(5) Toth, S., Huneau, D., Banrezes, B., and Ozil, J. P. (2006) Egg activation is the result of calcium signal summation in the mouse. *Reproduction 131*, 27–34.

(6) Kline, D., and Kline, J. T. (1992) Repetitive calcium transients and the role of calcium in exocytosis and cell cycle activation in the mouse egg. *Dev. Biol. 149*, 80–9.

(7) Tahara, M., Tasaka, K., Masumoto, N., Mammoto, A., Ikebuchi, Y., and Miyake, A. (1996) Dynamics of cortical granule exocytosis at fertilization in living mouse eggs. *Am. J. Physiol. 270*, C1354–61.

(8) Liu, J., and Maller, J. L. (2005) Calcium elevation at fertilization coordinates phosphorylation of XErp1/Emi2 by Plx1 and CaMK II to release metaphase arrest by cytostatic factor. *Curr. Biol. 15*, 1458–68.

(9) Madgwick, S., Hansen, D. V., Levasseur, M., Jackson, P. K., and Jones, K. T. (2006) Mouse Emi2 is required to enter meiosis II by reestablishing cyclin B1 during interkinesis. *J. Cell Biol. 174*, 791–801.

(10) Battaglia, D. E., and Gaddum-Rosse, P. (1987) Influence of the calcium ionophore A23187 on rat egg behavior and cortical F-actin. *Gamete Res. 18*, 141–52.

(11) Ozil, J. P. (1990) The parthenogenetic development of rabbit oocytes after repetitive pulsatile electrical stimulation. *Development 109*, 117–27.

(12) Zhang, D., Pan, L., Yang, L. H., He, X. K., Huang, X. Y., and Sun, F. Z. (2005) Strontium promotes calcium oscillations in mouse meiotic oocytes and early embryos through InsP3 receptors, and requires activation of phospholipase and the synergistic action of InsP3. *Hum. Reprod. 20*, 3053–61.

(13) Tingen, C., Rodriguez, S., Campo-Engelstein, L., and Woodruff, T. K. (2010) Research funding. Politics and parthenotes. *Science 330*, 453.

(14) Kim, A. M., Vogt, S., O'Halloran, T. V., and Woodruff, T. K. (2010) Zinc availability regulates exit from meiosis in maturing mammalian oocytes. *Nat. Chem. Biol. 6*, 674–81.

(15) Bernhardt, M. L., Kim, A. M., O'Halloran, T. V., and Woodruff, T. K. (2011) Zinc requirement during meiosis I-meiosis II transition in mouse oocytes is independent of the MOS-MAPK pathway. *Biol. Reprod. 84*, 526–36.

(16) Gee, K. R., Zhou, Z. L., Qian, W. J., and Kennedy, R. (2002) Detection and imaging of zinc secretion from pancreatic beta-cells using a new fluorescent zinc indicator. *J. Am. Chem. Soc. 124*, 776–8.

(17) Markoulaki, S., Matson, S., Abbott, A. L., and Ducibella, T. (2003) Oscillatory CaMKII activity in mouse egg activation. *Dev. Biol. 258*, 464–74.

(18) Fahrni, C. J., and O'Halloran, T. V. (1999) Aqueous coordination chemistry of quinoline-based fluorescence probes for the biological chemistry of zinc. *J. Am. Chem. Soc. 121*, 11448–11458.

(19) Konetschny-Rapp, S., Jung, G., Raymond, K. N., Meiwes, J., and Zahner, H. (1992) Solution thermodynamics of the ferric complexes of new desferrioxamine siderophores obtained by directed fermentation. *J. Am. Chem. Soc. 114*, 2224–2230.

(20) Colvin, R. A., Holmes, W. R., Fontaine, C. P., and Maret, W. (2010) Cytosolic zinc buffering and muffling: their role in intracellular zinc homeostasis. *Metallomics 2*, 306–17.

(21) Maret, W. (2011) Metals on the move: zinc ions in cellular regulation and in the coordination dynamics of zinc proteins. *Biometals* Epub ahead of print; DOI: 10.1007/s10534-010-9406-1.

(22) Nolan, E. M., and Lippard, S. J. (2009) Small-molecule fluorescent sensors for investigating zinc metalloneurochemistry. *Acc. Chem. Res. 42*, 193–203.

(23) Que, E. L., Domaille, D. W., and Chang, C. J. (2008) Metals in neurobiology: Probing their chemistry and biology with molecular imaging. *Chem. Rev. 108*, 1517–1549.Addendum: *Chem. Rev. 108*, 4328.

(24) Ducibella, T. (1996) The cortical reaction and development of activation competence in mammalian oocytes. *Hum. Reprod. Update 2*, 29–42.

(25) DiMaggio, A. J., Jr., Lonergan, T. A., and Stewart-Savage, J. (1997) Cortical granule exocytosis in hamster eggs requires microfilaments. *Mol. Reprod. Dev. 47*, 334–40.

(26) Wong, J. L., Koppel, D. E., Cowan, A. E., and Wessel, G. M. (2007) Membrane hemifusion is a stable intermediate of exocytosis. *Dev. Cell 12*, 653–9.

(27) Suzuki, T., Yoshida, N., Suzuki, E., Okuda, E., and Perry, A. C. (2010) Full-term mouse development by abolishing Zn^{2+}dependent metaphase II arrest without Ca^{2+} release. *Development 137*, 2659–2669.

(28) Taki, M., Wolford, J. L., and O'Halloran, T. V. (2004) Emission ratiometric imaging of intracellular zinc: design of a benzoxazole fluorescent sensor and its application in two-photon microscopy. *J. Am. Chem. Soc. 126*, 712–3.

(29) Longo, F. J., and Chen, D. Y. (1985) Development of cortical polarity in mouse eggs: involvement of the meiotic apparatus. *Dev. Biol. 107*, 382–94.

(30) Duncan, F. E., Moss, S. B., Schultz, R. M., and Williams, C. J. (2005) PAR-3 defines a central subdomain of the cortical actin cap in mouse eggs. *Dev. Biol. 280*, 38–47.

(31) Haugland, H. P. (2001) *Handbook of Fluorescent Probes and Research Chemicals*, 6th ed., Molecular Probes, Eugene, OR.

(32) Grynkiewicz, G., Poenie, M., and Tsien, R. Y. (1985) A new generation of Ca^{2+} indicators with greatly improved fluorescence properties. *J. Biol. Chem. 260*, 3440–50.

(33) Stork, C. J., and Li, Y. V. (2006) Intracellular zinc elevation measured with a "calcium-specific" indicator during ischemia and reperfusion in rat hippocampus: a question on calcium overload. *J. Neurosci. 26*, 10430–7.

(34) Shoji, S., Yoshida, N., Amanai, M., Ohgishi, M., Fukui, T., Fujimoto, S., Nakano, Y., Kajikawa, E., and Perry, A. C. (2006) Mammalian Emi2 mediates cytostatic arrest and transduces the signal for meiotic exit via Cdc20. *EMBO J. 25*, 834–45.

(35) Xu, M., West, E., Shea, L. D., and Woodruff, T. K. (2006) Identification of a stage-specific permissive in vitro culture environment for follicle growth and oocyte development. *Biol. Reprod. 75*, 916–23.

(36) Kramer, C. Y. (1956) Extension of multiple range tests to group means with unequal numbers of replications. *Biometrics 12*, 309–310.